HTML ABSTRACT + LINKS

JOURNAL OF APPLIED PHYSICS VOLUME 95, NUMBER 4 15 FEBRUARY 2004

# Dependence of the stress–temperature coefficient on dislocation density in epitaxial GaN grown on $\alpha$-$Al_2O_3$ and 6H–SiC substrates

I. Ahmad and M. Holtz[a]
*Department of Physics and NanoTech Center, Texas Tech University, Lubbock, Texas 79409*

N. N. Faleev[b] and H. Temkin
*Department of Electrical Engineering and NanoTech Center, Texas Tech University, Lubbock, Texas 79409*

(Received 16 September 2003; accepted 6 November 2003)

We report measurements of stress in GaN epitaxial layers grown on 6H–SiC and $\alpha$-$Al_2O_3$ substrates. Biaxial stresses span +1.0 GPa (tensile) to −1.2 GPa (compressive). Stress determined from curvature measurements, obtained using phase-shift interferometry (PSI) microscopy, compare well with measurements using accepted techniques of x-ray diffraction (XRD) and Raman spectroscopy. Correlation between XRD and Raman measurements of the $E_2^2$ phonon gives a Raman-stress factor of $-3.4\pm0.3\ \mathrm{cm}^{-1}/\mathrm{GPa}$. We apply PSI microscopy for temperature dependent stress measurements of the GaN films. Variations found in the stress–temperature coefficient correlate well with threading dislocation densities. We develop a phenomenological model which describes the thermal stress of the epitaxial GaN as a superposition of that for ideal GaN and the free volume existing in the layers due to the threading dislocations. The model describes well the observed dependence. © *2004 American Institute of Physics.* [DOI: 10.1063/1.1637707]

## I. INTRODUCTION

Gallium nitride is an important wide band-gap semiconductor for optoelectronic and high-power applications.[1,2] The epitaxial growth of GaN currently relies on the use of substrates $\alpha$-$Al_2O_3$ (sapphire)[3] and 6H–SiC (silicon carbide),[4] as well as silicon.[5] Although sapphire and SiC are the preferred substrate materials for GaN, heteroepitaxy leads to important problems related to stress. First, lattice constant mismatch of GaN with sapphire and SiC is −13% and +4%, respectively.[6] This mismatch leads to impractically small critical layer thickness values and ideal heteroepitaxy is not observed. Layers grown on these substrates are dense with threading and edge dislocations. Second, the thermal expansion coefficient in the basal plane of GaN differs significantly from those of SiC and sapphire.[7–10] Consequently, high-temperature deposition processes used in all epitaxial growth of GaN result in thermal stress upon cooling to room temperature, provided the material does not relax by cracking or on account of very high dislocation density. The biaxial stress observed in epitaxial GaN is, in general, a consequence of lattice constant and thermal mismatch strains.[11,12] Values can exceed 1 GPa, and are tensile for GaN grown on SiC (and Si) or compressive when using sapphire substrates.

Stress modulates the energy gap of GaN films[13,14] and, consequently, the optical properties. Extremely large values of stress can produce cracks[15–17] in these films. Consequently, the ability to examine stress in epilayers is essential to growth and device fabrication. In this study, we use samples with thickness up to 3.0 $\mu$m, so that relaxation is due to lattice constant and thermal expansion mismatches and dislocation,[18] and which exhibit no cracking.

The most direct approach for studying strain in epitaxial GaN is through x-ray diffraction (XRD) measurements.[19] The (0002) diffraction peak is used to determine the $c$-axis lattice constant and one off-axis diffraction measurement, such as $(11\bar{2}4)$, is needed to obtain the $a$-axis lattice constant. From these measurements, the strain is directly measured. Another accepted approach for obtaining biaxial stress in epilayers is Raman spectroscopy.[20] In GaN, the shift in the $E_2^2$ symmetry phonon energy, from the value exhibited by unstressed material, is proportional to the stress. These measurements are rapid and permit mapping with spatial resolution on the micron scale.[21] Raman stress assessment depends on the relationship between stress and phonon shift. For the $E_2^2$ phonon in GaN, different groups report Raman stress factors ranging from $-2.7\ \mathrm{cm}^{-1}/\mathrm{GPa}$ (Ref. 22) to $-7.7\ \mathrm{cm}^{-1}/\mathrm{GPa}$.[23] Raman scattering used to study the temperature dependence of stress in homoepitaxial layers are difficult to interpret. This is because the observed phonon shift is a superposition of the intrinsic (bulk) temperature dependence and a contribution arising from thermal expansion mismatch with the substrate. For XRD and Raman methods, it is critical to have accurate reference measurements of lattice constants and phonon energy, respectively. To relate strain to stress the elastic constants of GaN must be known.

In this article, we apply phase-shift interferometry (PSI) microscopy[24] to measure curvatures of epitaxially grown GaN layers for determining stress. These measurements rely on accurate values of Young's elastic moduli and the Poisson ratios of epilayers and substrate. For thin epitaxial layers, it is only necessary to know these constants for the substrate. We examine epilayers grown on both sapphire and SiC substrates so that biaxial compressive and tensile stress states

[a] Electronic mail: mark.holtz@ttu.edu
[b] Current address: Rigaku/MSC, Inc., 9009 New Trails Dr., The Woodlands, TX 77381.

 © 2004 American Institute of Physics

Downloaded 05 Feb 2004 to 129.118.86.46. Redistribution subject to AIP license or copyright, see http://jap.aip.org/jap/copyright.jsp

are studied. Results are directly compared with XRD and Raman measurements. We also report temperature dependent curvature/stress measurements on our samples using PSI. This is important since GaN-based devices locally heat under operation.[25] Variations observed in the stress–temperature coefficient are correlated with dislocation density.

## II. EXPERIMENT

We study two sets of GaN epilayers. In the first set of GaN grown on (0001) sapphire, molecular-beam epitaxy was initiated by a thin ($\sim$50 nm) AlN buffer layer grown on the substrate ($\sim$873 K). The substrate temperature was then elevated to $\sim$1080 K for growing the GaN epilayers. The second set was grown on 6H–SiC substrates at temperature $\sim$1290 K by hydride vapor phase epitaxy (HVPE). For the HVPE growth, no AlN buffer layer was used. The GaN layers range in thickness from 0.45 to 3.0 $\mu$m. GaN with a thickness of 25 $\mu$m on a Si substrate was used as a strain free reference sample for the Raman measurements.[26]

For the XRD measurements, a commercial system with a Ge(220), four-fold, Bartels-type monochromator and a Ge(220) three-fold analyzer was used for $2\theta$–$\omega$ scans and $\omega$ rocking curve. To measure the lattice constants of GaN, reflections of Cu $K\alpha_1$ line from (0002) planes in symmetrical mode and $(11\bar{2}4)$ planes in asymmetrical mode were observed. Reflections with planes (0004), (0006), and $(10\bar{1}5)$ were also analyzed. The strain components along the wurtzite $c$ axis ($\varepsilon_{zz}$), and along $a=b$ axis ($\varepsilon_{xx}$) are calculated by $\varepsilon_{zz}=(c-c_0)/c_0$ and $\varepsilon_{xx}=(a-a_0)/a_0$, where $c_0$ and $a_0$ are lattice constants of fully relaxed GaN.[27]

Light from an $Ar^+$-ion laser (488 nm) was focused onto the sample surface for the micro-Raman studies. The scattered radiation was analyzed by 0.5 m spectrometer and detected using a liquid-$N_2$-cooled charged coupled device array. The system was precisely calibrated with spectral lines from a Ne lamp and the argon plasma lines. The spectral resolution of the system was 2.0 $cm^{-1}$ and precision was 0.2 $cm^{-1}$. The measurements were performed in backscattering mode with incident light along (0001) direction of GaN films for which the $E_2^2$ symmetry phonon is Raman active.

A commercial interferometric microscope in PSI mode was used to measure the curvature of GaN films. White light is filtered and passed through an interferometer objective for focusing on the wafer. A beam splitter directs half of the light to a reference surface and half to the sample. Reflections from the GaN and reference surfaces are combined to form interference fringes. Relative motion of the sample by small known amounts along the optical axis, with the help of a piezoelectric transducer, introduces a phase shift between objective and reference beam. Integration of intensity data is the wave front or phase. The phase data for the circular field of view of the samples are processed pixel by pixel and relative surface height, is calculated using $h(x,y)=\lambda/4\pi\phi(x,y)$, where $\lambda=630$ nm is the wavelength of the source beam and $\phi(x,y)$ is the phase data.[24]

Curvature was studied as a function of temperature. A heating stage was positioned under the PSI microscope, with range from room temperature to $\sim$100 °C. The temperature at the surface of the wafer (i.e., at the epilayers) was determined by fixing a commercial RTD on an identical substrate positioned next to the sample under study. A closed-loop proportional integral differential controller was used to maintain constant temperature with the RTD value as feedback.

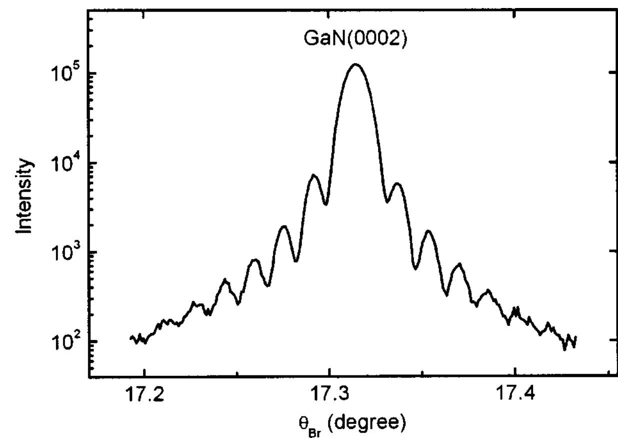


FIG. 1. Typical XRD $2\theta$-$\omega$ data for GaN grown on SiC.

## III. COMPARISON OF X-RAY DIFFRACTION, RAMAN, AND PHASE-SHIFT INTERFEROMETERY STRESS MEASUREMENTS

Figure 1 shows representative XRD results for a GaN layer grown on SiC. The sharpness of the peak demonstrates high crystalline quality and presence of the Pendellösung fringes confirms the GaN surface flatness. The threading dislocation density is obtained using the measured linewidth and Scherer's relation. Diffraction angles of the (0002) allow us to obtain the $c$-axis lattice constant and $\varepsilon_c$, and this together with measurement of the $(11\bar{2}4)$ diffraction band allow us to obtain the $a$-axis parameter and $\varepsilon_a$. We calculated the Poisson ratio $\nu$ from

$$\varepsilon_c/\varepsilon_a=-2\nu/(1-\nu) \tag{1}$$

and biaxial stress $\sigma$ using

$$\varepsilon_a=\frac{1-\nu}{E}\sigma, \tag{2}$$

and

$$\varepsilon_c=-\frac{2\nu}{E}\sigma, \tag{3}$$

where $E$ is Young's modulus. The Poisson ratio gives excellent consistency with average value of $\nu=0.20\pm0.02$. This agrees well with published values of the Poisson ratio.[11,28,29] The value of stress was calculated using our Poisson ratio and Young's modulus, $E=290$ GPa, from Refs. 11, 28, and 29.

Stress in epitaxial GaN(0001) is biaxial. The Raman shift $\Delta\omega$ from the phonon energy of the unstressed material is related to biaxial stress according to $\sigma=\Delta\omega/k_R$, where $k_R$ is Raman stress factor. We adopt the convention that $\sigma>0$ ($<0$) corresponds to tensile (compressive) stress. Figure 2

Downloaded 05 Feb 2004 to 129.118.86.46. Redistribution subject to AIP license or copyright, see http://jap.aip.org/jap/copyright.jsp

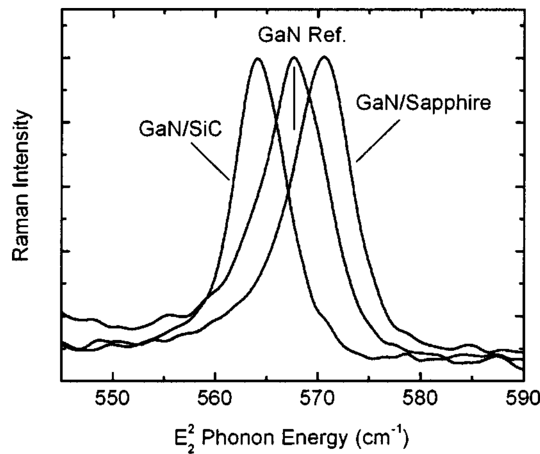


FIG. 2. Representative Raman spectra showing the shift in energy of the $E_2^2$-symmetry phonon, from that of unstressed GaN. Blueshift results from compressive stress (GaN/sapphire) and redshift is from tensile stress (GaN/SiC).

shows the red- and blueshifts of $E_2^2$ phonon due to compressive stress (GaN on sapphire) and tensile stress (GaN on SiC), respectively. The relationship between strain and the Raman shift can be written as

$$\frac{\varepsilon_c}{\Delta\omega} = -E^{-1} 2\nu/k_R, \tag{4}$$

where $\varepsilon_c/\Delta\omega$ is referred to as the Raman strain factor. Thus, XRD is used to obtain strain values and Raman scattering used to obtain associated shifts in the phonon energy.

Correlation between strain (XRD measurements) in GaN films and Raman shift of $E_2^2$ phonon is illustrated in Fig. 3. Here, we show results for both large tensile and compressive biaxial stresses, inducing large strains and phonon shifts. Despite the scatter, a single linear fit describes well the overall trend. Table I gives the values of Raman stress factor from Eq. (4), using Poisson ratio and Young's modulus from different sources, and the Raman strain factor obtained from a linear fit to the data in Fig. 3. Values range from $-3.1\ \mathrm{cm}^{-1}$/GPa to $-4.2\ \mathrm{cm}^{-1}$/GPa. Using $E = 290$ GPa (Refs. 11, 28, and 29) and $\nu = 0.20$ obtained here, we obtain $k_R = -3.4 \pm 0.3\ \mathrm{cm}^{-1}$/GPa. Our value of the GaN Raman stress factor is in the range of published values $-2.7$,[22] $-4.1$,[33] $-6.2$,[34] and $-7.7$ GPa.[23] Our measurements establish correlation between Raman phonon shift and both strain and stress from XRD measurements. The $k_R$ value for AlN based on combined Raman and XRD measurements is reported to be $k_R = 6.3 \pm 1.4\ \mathrm{cm}^{-1}$/GPa.[35]

In a layered structure, stress induces warping of the epilayers and substrate. We apply the model of Olson and Ettenberg[36] for calculating stress in a layered structure. We neglect effects of the buffer layer because it is very thin and since the elastic constants of AlN are similar to those of GaN.[37] For a two layer structure consisting of substrate (subscript 1), and film (subscript 2), with Young's moduli $E_i$, Poisson ratios $\nu_i$, and thickness $t_i$, the biaxial stress is

$$\sigma = \frac{(E_1 t_1^3 + E_2 t_2^3)}{6(1-\nu_1)(t_1+t_2)t_2}\frac{1}{R} \approx \frac{E_1 t_1^2}{6(1-\nu_1)t_2}\frac{1}{R}, \tag{5}$$

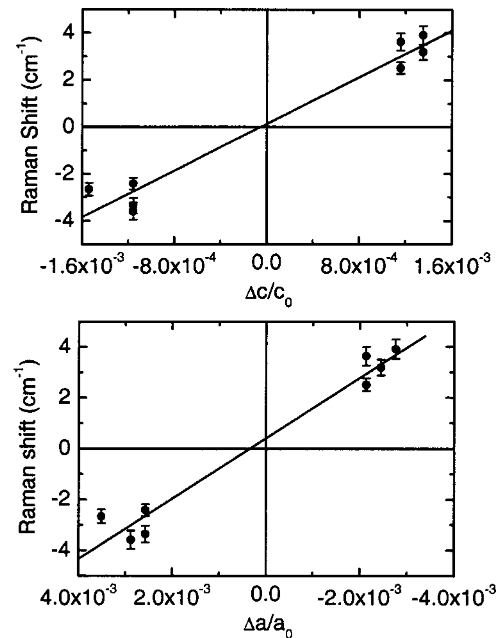


FIG. 3. Raman shift of $E_2^2$ phonon vs strain along $c$ axis (upper panel) and $a$ axis (lower panel).

where $R$ is the measured radius of curvature due to warping. The approximation in Eq. (5) is valid when $t_2 \ll t_1$, which is generally the case for epitaxially grown layers. Under these conditions, the elastic constants of the substrate only are needed. For the samples investigated here, the difference between the equality in Eq. (5) and the approximation is $<1\%$; here, we use the equality. Figure 4 shows sample PSI measurements for GaN grown on sapphire [Fig. 4(a)] and SiC [Fig. 4(b)] substrates. Samples are curved according to type of stress in the epilayer: Convex curvature is related to compressive stress [Fig. 4(a)] and concave curvature connotes tensile stress [Fig. 4(b)]. Parameters used to calculate the biaxial stress using curvature measurements are given in Table II. Epilayer thickness values were determined by scanning electron microscope cross section and optical reflectivity.[39]

In Fig. 5, we establish the correlation between stress measurements carried out using PSI microscopy curvature determination and both XRD and Raman spectroscopy. The dashed line in Fig. 5 is the desired direct correspondence. Deviation between the ideal correspondence and the data is

TABLE I. Constants used for Raman stress factor and resulting $k_R$.

| $E$ (GPa) | $\nu$ | $k_R$ ($\mathrm{cm}^{-1}$/GPa) |
|---|---|---|
| 314[a] | 0.24[a] | $-3.8 \pm 0.3$ |
| 324[b] | 0.20[b] | $-3.1 \pm 0.3$ |
| 305[c] | 0.26[c] | $-4.2 \pm 0.3$ |
| 290[d] | $0.23 \pm 0.06$[d] | $-4.0 \pm 0.3$ |
| 290[d] | $0.20 \pm 0.02$[e] | $-3.4 \pm 0.3$ |

[a]See Ref. 30.
[b]See Ref. 31.
[c]See Ref. 28.
[d]See Refs. 11 and 32.
[e]This work.

Downloaded 05 Feb 2004 to 129.118.86.46. Redistribution subject to AIP license or copyright, see http://jap.aip.org/jap/copyright.jsp

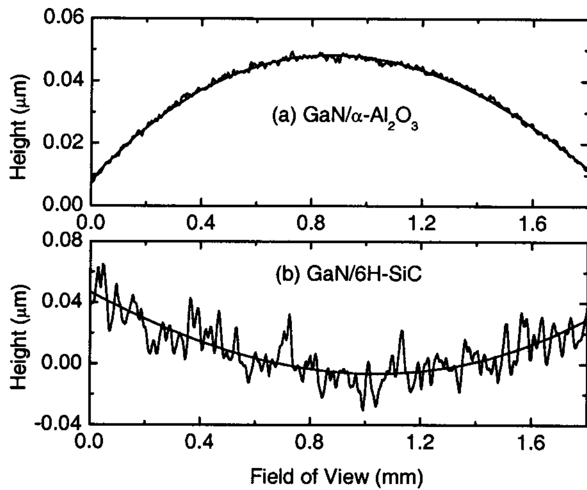


FIG. 4. Example curvature measurements from PSI. (a) Convex curvature ($R<0$) due to compressive stress from the sapphire substrate. (b) Concave curvature ($R>0$) due to tensile stress for SiC Substrate.

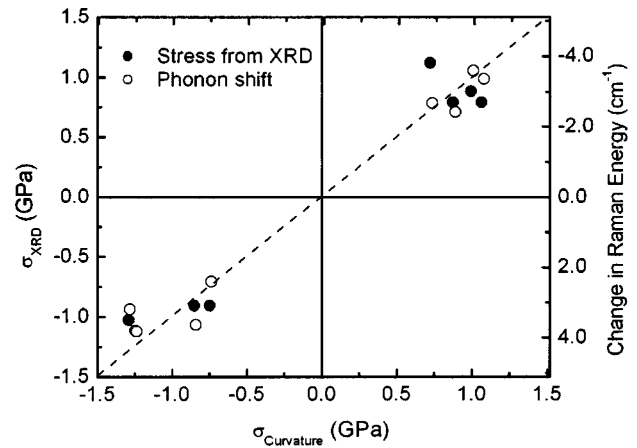


FIG. 5. Comparison of the methods used to determine stress: XRD vs curvature (filled circles), and Raman shift vs curvature (open circles). Note the reversed scale on the right-hand side Raman axis. The correlation between Raman shift and XRD is implied from Fig. 3 and this figure. The dashed line corresponds to ideal agreement.

attributable to differences in the measurement techniques. XRD will be most sensitive to strain (stress) near the surface of the wafer. Raman measurements will average stress throughout the entire depth of focus ($\sim 2\ \mu$m) corresponding to the epilayers thickness. Curvature will depend on epilayer–interface stress, and thus be more sensitive to this region. Finally, the dislocation density in the GaN varies with layer thickness and distance from the substrate, exhibiting close correlation with Raman stress measurements.[40] All of these factors will produce deviations between the various approaches to measuring stress. Clearly, agreement is excellent over the wide range of stresses examined here. These comparisons clearly establish consistency between PSI-based curvature measurements for stress analysis in GaN films and the accepted XRD and Raman spectroscopy methods.

## IV. TEMPERATURE DEPENDENCE OF STRESS

We now apply the PSI measurements to examine the effect of heating on the epilayer stress. A similar study has been reported on important coatings on glass substrates.[24] We used PSI for stress measurements of GaN on sapphire and SiC substrates for temperatures ranging between 20 and 100 °C. Representative results are shown in Figs. 6(a) and 6(b) for GaN on sapphire and SiC substrates, respectively. The total measured stress at an arbitrary temperature is given by[41]

$$\sigma=\sigma_i+\sigma_{\mathrm{th}}, \tag{6}$$

TABLE II. Parameters used in the calculation of stress by curvature measurement.

| Parameter | $\alpha$-$Al_2O_3$ | 6H–SiC | GaN |
|---|---|---|---|
| Thickness ($\mu$m) | 300 | 200 | 0.5–3.0 |
| Young's modulus (GPa) | 345[a] | 180[b] | 290 |
| Poisson ratio | 0.28[a] | 0.18[b] | 0.20±0.02 |

[a]See Ref. 29.
[b]See Ref. 38.

where $\sigma_i$ is intrinsic stress and $\sigma_{\mathrm{th}}$ is thermal stress

$$\sigma_{\mathrm{th}}=\frac{E_2}{(1-\nu_2)}(\alpha_1-\alpha_2)(T-T_0), \tag{7}$$

with $\alpha_1$ and $\alpha_2$ as the thermal expansion coefficients of substrate and GaN films, respectively. $T_0$ is the growth temperature. For GaN, sapphire, and SiC, the expansion coefficients are $\alpha_{\mathrm{SiC}}<\alpha_{\mathrm{GaN}}<\alpha_{\mathrm{sapphire}}$. Figure 6 thus shows the expected reduction in the biaxial stress magnitude with increasing temperature for GaN on each substrate. This suggests that the stress is small at the growth temperature, in accordance with Eq. (6), a topic we will return to later. Choosing the temperature range judiciously, such that $\alpha_i$ are approximately constant, then

$$\frac{d\sigma_{\mathrm{th}}}{dT}=\frac{E_2}{(1-\nu_2)}(\alpha_1-\alpha_2). \tag{8}$$

The quantity $d\sigma/dT(=d\sigma_{\mathrm{th}}/dT)$ is obtained from the slope of data as shown in Fig. 6.

By measuring epilayers with different thickness, and on both substrate types, we observe deviations in $d\sigma_{\mathrm{th}}/dT$. Since the substrates are expected to have well-defined thermal expansion coefficients, we attribute the deviations seen in films on the same substrate to differences in the GaN layer. In Fig. 7, we graph measured $d\sigma/dT$ versus threading dislocation (TD) density $n$, for GaN grown on sapphire (a) and SiC (b). The TD density values are from XRD measurements.[40] The GaN/SiC case clearly supports a direct dependence between the stress–temperature coefficient and dislocation density. For GaN/sapphire we also adopt a linear relationship as the simplest interpretation.

In the spirit of Ref. 30, we introduce a strain mechanism associated with the presence of defects. In our case, the dominant defects which correlate to stress relaxation are threading dislocations,[40] which introduce free volume into the crystal. Assuming a strain in direct proportion to $n$

$$\varepsilon_{\mathrm{TD}}=L_0^2 n, \tag{9}$$

Downloaded 05 Feb 2004 to 129.118.86.46. Redistribution subject to AIP license or copyright, see http://jap.aip.org/jap/copyright.jsp

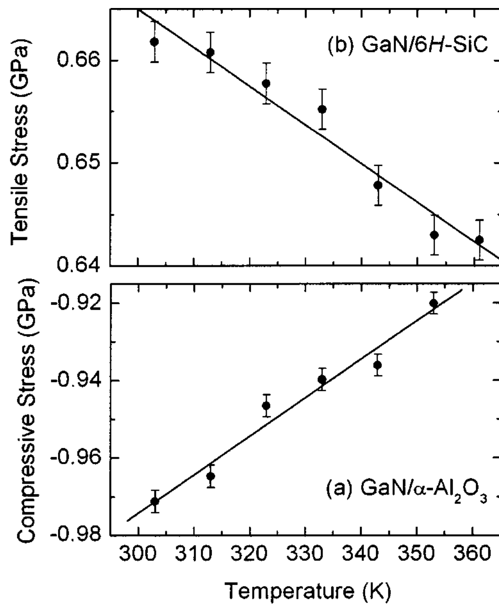


FIG. 6. Representative temperature dependence of stress determined using the measured curvature. (a) GaN on sapphire. (b) GaN on SiC substrate. The lines correspond to linear least-squares fits. Error in the epilayers temperature is $\pm 2$ K.

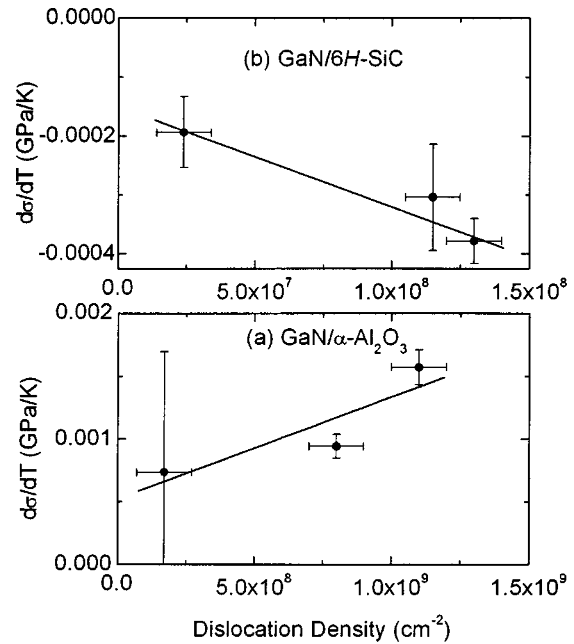


FIG. 7. Dependence of fitted slopes to data as in Fig. 6 ($d\sigma/dT$) on dislocation density from XRD for GaN. (a) Sapphire substrate. (b) SiC substrate. The lines are linear least-squares fits to the data.

where $L_0$ is a length parameter related to the range surrounding a TD over which stress relaxation occurs. The strain in the epilayer perpendicular to the growth $c$ axis is then

$$\varepsilon_a = (1 - L_0^2 n)\left\{1 + \frac{(1-\nu_2)}{E_2}\sigma\right\} - 1, \tag{10}$$

where $\sigma$ is the biaxial stress. From this, and using $d\varepsilon/dT = (\alpha_1 - \alpha_2)$ which is consistent with Eq. (8), we obtain

$$\frac{d\sigma}{dT} = \frac{E_2}{1-\nu_2}\frac{(\alpha_1-\alpha_2)}{(1-L_0^2 n)} \approx \frac{E_2}{1-\nu_2}(\alpha_1-\alpha_2)(1+L_0^2 n), \tag{11}$$

where the approximation holds whenever $L_0^2 n \ll 1$. As in Eq. (8), we assume the expansion coefficients to be nearly constant over the temperature range of interest. Equations (10) and (11) reduce to Eqs. (2) and (8), respectively, when $n = 0$. The differences in sign obtained for $d\sigma/dT$ in Figs. 7(a) and 7(b) are due to the ordering of the thermal expansion coefficients discussed in relation to Eq. (7). The model also preserves the signs of the stress and expected stress–temperature coefficient due to the effects of either tensile or compressive stress on the open volume associated with TDs. We thus arrive at a linear dependence between the stress–temperature coefficient and $n$. The quantity $\alpha_2$ is the expansion constant of GaN with zero-TD density.

Based on this straightforward model, we can now interpret the dependence seen in Fig. 7. A linear fit is shown in Figs. 7(a) and 7(b). The intercept corresponds to the coefficient of unity in Eq. (11). Using the elastic parameters for GaN from Table I, and the substrate expansion coefficients near room temperature from Refs. 7 and 8, we obtain values of $\alpha_2$ for "perfect" GaN. These values are $(2.9 \pm 1.9) \times 10^{-6}\ \mathrm{K}^{-1}$ from our GaN/sapphire measurements [Fig. 7(a)] and $(3.1 \pm 1.0) \times 10^{-6}\ \mathrm{K}^{-1}$ for our GaN/SiC case [Fig. 7(b)]. The error ranges quoted here are conservatively large. Uncertainties arise from several sources. Experimentally, there are uncertainties in measuring the XRD-based TD density, curvature, and the sample temperature. Additionally, the XRD measures a lateral average property over a $\sim 2$ mm $\times 10$ mm probe area, while the field of view of the PSI microscope is $\sim 1.8$ mm in diameter. Since it is possible for stress to vary across a wafer, differences in positioning of the probes will introduce error. More importantly, we assume in this analysis that the TD density is uniform along the growth axis. Our work on GaN/SiC, using reciprocal space mapping for different Bragg reflections, corresponding to different probe depths, indicates that the TD density varies significantly for different epilayer thicknesses and along the growth axis.[40] This will influence both the reported TD density and the stress present in the epilayers. Despite these limitations, the values of $\alpha_2$, representative of GaN free of TDs, are consistent from the studies presented here on two distinctly different substrates. We find published values for the linear expansion coefficient of GaN: $2.8 \times 10^{-6}\ \mathrm{K}^{-1}$ (300 K),[8] $5.59 \times 10^{-6}\ \mathrm{K}^{-1}$ (300–900 K),[10] and $3.7 \times 10^{-6}\ \mathrm{K}^{-1}$ (300 K).[9] Our result best agrees with the value in Ref. 8, which is measured for a bulk sample of GaN. The large disagreement seen with the value in Ref. 10 most likely stems from the fact that the expansion coefficient increases with temperature, and they report an average value. We point out that this commonly used expansion coefficient for GaN is not valid near room temperature. Furthermore, it is clear from our results that the quality of the GaN will have a strong impact on thermal stress.

The slopes of the fits in Fig. 7 correspond to the coefficient of $n$ in Eq. (11). Eliminating the common prefactor of the slope and intercept from the fit results gives us values of $L_0 = 1.1 \pm 0.7\ \mu$m for the GaN/SiC data and $0.4 \pm 0.3\ \mu$m for

Downloaded 05 Feb 2004 to 129.118.86.46. Redistribution subject to AIP license or copyright, see http://jap.aip.org/jap/copyright.jsp

the GaN/sapphire case. The error stems from the same sources as above. As mentioned, $L_0$ corresponds to the distance over which the stress relaxation expected near TD decays. The 1 $\mu$m order of magnitude agrees well with finite element simulations of stress relaxation near cracks in GaN and AlN.[16] The model presented here, in relation to Eq. (11), is valid when $L_0^2 n \ll 1$. With the value of $L_0$ determined, this implies that epilayers with TD densities well below $10^{10}$ cm$^{-2}$ will fall within this range of validity.

## V. SUMMARY

We correlate independent measures of strain and stress on epitaxial GaN grown on sapphire (compressive) and SiC (tensile) substrates. From XRD measurements of both (0002) and $(11\bar{2}4)$ Bragg peaks, we obtain the lattice constants of GaN along the $a$ and $c$ directions. Using published lattice constants for unstrained GaN, we obtain strain along the $a$ axis ($\varepsilon_{xx}$) and $c$ axis ($\varepsilon_{zz}$). Using these strain values, we obtain GaN Poisson ratio $\nu = 0.20 \pm 0.02$. Raman measurements of the same wafers allow us to correlate strain with the $E_2^2$ phonon shift (Fig. 3). Using a published value of the GaN Young's modulus, we obtain Raman stress factor $-3.4 \pm 0.3$ cm$^{-1}$/GPa by directly correlating XRD and Raman measurements. Stress in the GaN films is also determined by from curvature measurements using PSI. The three quantities, strain from XRD, stress from curvature, and phonon shift are found to be consistent (Fig. 5).

We apply the curvature-based stress determination to study the effect of temperature, between 20 and 100 °C, on stress in GaN films. We observe that stress decreases linearly as temperature is raised over this range (Fig. 6). This stress reduction is due to the differences in thermal expansion coefficients of the substrate and epilayers. We observe that the stress–temperature coefficient $d\sigma/dT$ varies noticeably between samples grown on each type of substrate (Fig. 7). These variations are correlated with the TD density obtained from XRD linewidth analysis. We develop a model which accounts for the free volume associated with TDs to explain the observed trend in the stress–temperature coefficient. The model naturally accounts for contraction (expansion) around the TD due to compressive (tensile) stress.

## ACKNOWLEDGMENTS

The authors would like to thank Y. Melnik and V. Demitriev of TDI for the GaN/SiC samples used in this study. They also acknowledge support from the National Science Foundation (ECS-0304224, CNCI-0330348, and ECS-0323640), DARPA-SUVOS (Dr. J. Carrano), and the J. F. Maddox Foundation.

[1] S. J. Pearton, J. C. Zolper, R. J. Shul, and F. Ren, J. Appl. Phys. **86**, 1 (1999).
[2] S. C. Jain, M. Willander, J. Narayan, and R. Van Overstraeten, J. Appl. Phys. **87**, 965 (2000).
[3] H. Morkoc, S. Strite, G. B. Gao, M. E. Lin, B. Sverdlov, and M. Burns, J. Appl. Phys. **76**, 1363 (1994).
[4] F. A. Ponce, B. S. Krusor, J. S. Major, Jr., W. E. Plano, and D. F. Welch, Appl. Phys. Lett. **67**, 410 (1995).
[5] S. A. Nikishin, N. N. Faleev, V. G. Antipov, S. Francoeur, L. Grave de Peralta, G. A. Seryogin, H. Temkin, T. Prokofyeva, M. Holtz, and S. N. G. Chu, Appl. Phys. Lett. **79**, 2073 (1999).
[6] F. A. Ponce, D. P. Bour, W. Götz, N. M. Jonson, H. I. Helava, I. Grzegory, and S. Porowski, Appl. Phys. Lett. **68**, 917 (1996).
[7] V. Kirchner, H. Heinke, D. Hommel, J. Z. Domagala, and M. Leszczynski, Appl. Phys. Lett. **77**, 1434 (2000).
[8] M. Leszczynski, T. Suski, H. Teisseyre, P. Perlin, I. Grzegory, J. Jun, S. Porowski, and T. D. Moustakas, J. Appl. Phys. **76**, 4909 (1994).
[9] A. U. Sheleg and V. A. Savastenko, Ser. Fiz. Mat. Nauk **3**, 126 (1976).
[10] Landolt–Bornstein (Springer, New York, 1982).
[11] T. Detchprohm, K. Hiramatsu, K. Itoh, and I. Akasaki, Jpn. J. Appl. Phys., Part 2 **31**, L1456 (1992).
[12] J. Neugebaur and C. G. Van de Walle, Phys. Rev. B **50**, 8067 (1994).
[13] B. Gil, in *Gallium Nitride II*, edited by J. I. Pankove and T. D. Moustakas (Academic, Boston, 1999), Vol. 57.
[14] W. Rieger, T. Metzger, H. Angerer, R. Dimitrov, O. Ambacher, and M. Stutzmann, Appl. Phys. Lett. **68**, 970 (1996).
[15] L. T. Romano, C. G. Van de Walle, J. W. Ager, W. Götz, and R. S. Kern, Appl. Phys. Lett. **87**, 7745 (2000).
[16] C. Ramkumar, T. Prokofyeva, M. Seon, M. Holtz, K. Choi, J. Yun, S. A. Nikishin, and H. Temkin, MRS Internet J. Nitride Semicond. Res. **693**, I3.55.1 (2002).
[17] J. Han, K. E. Waldrip, S. R. Lee, J. J. Figiel, S. J. Hearne, G. A. Petersen, and S. M. Myers, Appl. Phys. Lett. **78**, 67 (2001).
[18] K. Hiramatsu, T. Detchprohm, and I. Akasaki, Jpn. J. Appl. Phys., Part 1 **32**, 1528 (1993).
[19] H. Heinke, V. Kirchner, S. Einfeldt, and D. Hommel, Appl. Phys. Lett. **77**, 2145 (2000).
[20] R. Liu and N. Cave, in *SiGeC Alloys and their Applications*, edited by S. Pantelides and S. Zollner (Gordon and Breach, New York, 2002).
[21] M. Holtz, M. Seon, T. Prokofyeva, H. Temkin, R. Singh, F. P. Dabkowski, and T. D. Moustakas, Appl. Phys. Lett. **75**, 1757 (1999).
[22] V. Y. Davydov, N. S. Averkiev, I. N. Goncharuk, D. K. Nelson, I. P. Nikitina, A. S. Polkovnikov, A. N. Smirnov, M. A. Jacobson, and O. K. Semchinova, J. Appl. Phys. **82**, 5097 (1997).
[23] I. Lee, I. Choi, C. Lee, E. Shin, D. Kim, S. K. Noh, S. Son, J. Y. Lim, and H. J. Lee, J. Appl. Phys. **83**, 5787 (1998).
[24] C. C. Lee, C. L. Tien, W. S. Sheu, and C. C. Jaing, Rev. Sci. Instrum. **72**, 2128 (2001).
[25] R. Gaska, A. Osinsky, J. W. Yang, and M. S. Shur, IEEE Electron Device Lett. **19**, 89 (1998).
[26] M. Seon, T. Prokofyeva, M. Holtz, S. A. Nikishin, N. N. Faleev, and H. Temkin, Appl. Phys. Lett. **76**, 1842 (2000).
[27] M. Leszczynski, H. Teisseyre, T. Suski, I. Grzegory, M. Bockowski, J. Jun, S. Porowski, K. Pakula, J. M. Baranowski, C. T. Foxon, and T. S. Cheng, Appl. Phys. Lett. **69**, 73 (1996).
[28] A. Polian, M. Grimsditch, and I. Grzegory, J. Appl. Phys. **79**, 3343 (1996).
[29] J. B. Wachman, W. E. Tefft, D. E. Lam, and R. P. Stinchfield, J. Res. Natl. Bur. Stand. **64A**, 213 (1960).
[30] K. Kim, W. R. L. Lambrecht, and B. Segall, Phys. Rev. B **50**, 1502 (1994).
[31] T. Azuhata, T. Sota, and K. Suzuki, J. Phys.: Condens. Matter **8**, 3111 (1996).
[32] M. Leszczynski, T. Suski, H. Teisseyre, I. Grzegory, M. Bockowski, J. Jun, S. Porowski, and J. Major, J. Phys. D **28**, L149 (1995).
[33] C. Kisielowski, J. Krüger, S. Ruvimov, T. Suski, J. W. Ager, E. Jones, Z. Liliental-Weber, M. Rubin, E. R. Weber, M. D. Bremser, and R. F. Davis, Phys. Rev. B **54**, 17745 (1996).
[34] T. Kozawa, T. Kachi, H. Kano, Y. Taga, M. Hashimoto, N. Koide, and K. Manabe, J. Appl. Phys. **75**, 1098 (1994).
[35] T. Prokofyeva, M. Seon, J. Vanbuskirk, M. Holtz, S. A. Nikishin, N. N. Faleev, H. Temkin, and S. Zollner, Phys. Rev. B **63**, 125313 (2000).
[36] G. H. Olson and M. Ettenberg, J. Appl. Phys. **48**, 2543 (1977).
[37] M. E. Sherwin and T. D. Drummond, J. Appl. Phys. **69**, 8423 (1991).
[38] R. G. Munro, J. Phys. Chem. Ref. Data **26**, 1195 (1997).
[39] M. Holtz, T. Prokofyeva, M. Seon, K. Copeland, J. Vanbuskirk, S. Williams, S. Nikishin, V. Tretyakov, and H. Temkin, J. Appl. Phys. **89**, 7977 (2001).
[40] N. Faleev, I. Ahmad, M. Holtz, and H. Temkin (unpublished).
[41] C. J. Sun, P. Kung, A. Saxler, H. H. K. Ohsato, and M. Razeghi, J. Appl. Phys. **75**, 3964 (1994).

**Downloaded 05 Feb 2004 to 129.118.86.46. Redistribution subject to AIP license or copyright, see http://jap.aip.org/jap/copyright.jsp**